First-principles norm-conserving pseudopotential with explicit incorporation of semicore states

Carlos L. Reis,[1] J. M. Pacheco,[1,2] and José Luís Martins[3]
[1]*Centro de Física Teórica e Computacional, Complexo Interdisciplinar da Universidade de Lisboa, Av. Prof. Gama Pinto 2, P-1649-003 Lisboa Codex, Portugal*
[2]*Departamento de Física da Faculdade de Ciências, Complexo Interdisciplinar da Universidade de Lisboa, Av. Prof. Gama Pinto 2, P-1649-003 Lisboa Codex, Portugal*
[3]*Departamento de Física, Instituto Superior Técnico, Av. Rovisco Pais, 1049-001 Lisboa, Portugal and INESC-MN, Rua Alves Redol 9, 1000-029 Lisboa, Portugal*
(Received 8 February 2003; revised manuscript received 21 April 2003; published 15 October 2003)

We develop a pseudopotential generation scheme which provides, in a systematic way, first-principles, transferable, norm-conserving pseudopotentials which include, in addition to standard valence electrons, semicore electrons. The scheme improves the quality of the pseudopotential for some transition metal polyatomic systems where the semicore states can play an active role in the chemical bonding of those systems. The method is employed to generate pseudopotentials for Ti and Cu, taken as limiting examples of $3d$ transition metals, which are then used to study the structural properties of both homonuclear dimers and the bulk solid of these elements. The results obtained put in evidence the excellent agreement obtained in all cases between the pseudopotential results and benchmark all-electron calculations for the same systems.

DOI: 10.1103/PhysRevB.68.155111 PACS number(s): 71.15.Dx, 71.20.Be, 31.15.−p

I. INTRODUCTION

Electronic-structure calculations performed within the framework of density functional theory (DFT) in its different approximation flavors, have demonstrated their capacity not only to describe accurately but also to predict, different physical and chemical properties of complex molecular liquid and solid state systems, ranging from phase transitions, defects in semiconductors, structural and electronic properties of atomic clusters, the structure of and diffusion on surfaces, as well as the electromagnetic excitations in molecules and solids. In many of these applications use has been made of pseudopotentials.

Replacing the effect that chemically inert core states exert on the chemically active valence states by means of an effective pseudopotential dates back to the early work of Fermi[1] and Phillips and Kleinman,[2] and has seen a sizeable amount of interest and further improvements since the development of norm-conserving pseudopotentials.[3–5] The physical reasoning behind the pseudopotential approximation is simple: Since the core electron wave functions of an atom remain essentially unchanged when placed into different chemical environments and since to a large extent the contribution of the core wave functions to chemical bonding is to enforce the orthogonality between the valence wave functions and the core states, the true atomic potential can indeed be replaced by a pseudopotential that reproduces the effects of the core electrons. As a result, transferable *ab initio* pseudopotentials[6–9] have been successfully developed and used in band structure and total-energy calculations for complex polyatomic systems.[10] For calculations with a plane wave (PW) basis set, a pseudopotential that gives a fast convergence of the calculated properties with increasing basis set size is commonly called a ''soft'' pseudopotential.[11] Due to the popularity of PW calculations a great deal of effort has been made in identifying the characteristics of softness in a pseudopotential, and in developing new generation methods that produce softer pseudopotentials. An example of such a type of soft pseudopotential is the Troullier and Martins (TM) pseudopotential[8] which allows the numerical simulation of complex systems to be carried out with significant savings of memory and computing time, and which we generalize in the present work in order to incorporate semicore states (see below).

One can easily generate a TM for any element of the periodic table. For most elements and applications this pseudopotential is very accurate in the sense that the error associated with replacing the cores by a pseudopotential is significantly smaller than the error introduced by replacing the exact exchange and correlation by an approximate functional such as the local density approximation (LDA). In other words, the difference between similar pseudopotential and all-electron (AE) calculations is smaller than the difference between AE and experiment. There are, however, a few cases where the pseudopotential approximation is not satisfactory and an even smaller number of cases where it fails. Those cases correspond to atoms where the basic assumption of the pseudopotential approximation—that the core and valence electron wave functions are well separated in both space and momentum—is not well verified, that is, when the core states have a large extension or are not strongly bound. Such states are called semicore states. Situations for which the predictions of usual pseudopotentials such as the TM fail are the bond lengths of titanium, vanadium, or chromium dimers and small clusters.[12] These $3d$ transition metal dimers have a surprisingly short bond length. For instance, the distance between atoms in Ti_2 is only 65% of the nearest neighbor distance in the bulk metal, and the type of bonding is truly exotic (δ bonds). Another (albeit related) situation is the lack of accuracy in the quasiparticle calculations of electronic energies and lifetimes of transition metals.[13] Indeed, these are situations in which the role of semicore electrons—that is, those electrons in the completely filled shells below the valence shell—cannot be ignored, and indeed several

methods have been proposed which allow the inclusion of semicore electrons as active in the pseudopotential.[14,15]

The problem with the $3d$ transition metals is that their valence configuration is $4s^n4p^03d^m$, and due to the lack of d electrons in the core the $3d$ wave functions are compact and overlap significantly with the $3s$ and $3p$ semicore states. This effect is larger in the early elements of the series where those semicore states are less bound and more extended. An obvious solution would be to include those $3s$ and $3p$ semicore states as part of the valence in the pseudopotential generation scheme. That would require only a somewhat larger energy cutoff in the plane-wave expansion with respect to the $3d$ electrons and a larger number of electrons in the valence, corresponding to a manageable increase in the necessary computing resources. For a large class of pseudopotentials, however, such a generalization is not possible for a technical reason, namely, if a screened pseudopotential is generated by inverting the Schrödinger equation for a pseudo-wave-function then the procedure is valid only for nodeless pseudo wave functions, and one can only have a single pseudo-wave-function of a given orbital with quantum number l, in order to warrant its nodeless structure. As the $4p$ orbitals are unoccupied one can easily include the $3p$ electrons in those class of schemes by considering a $3p^64s^n3d^m$ valence configuration. However, in this way one treats the $3s$ and $3p$ electrons on a different footing, a feature which is not easy to justify. One can also generate pseudopotentials from an ionized configuration $3s^23p^63d^m$ (implying $4s^0$), but pseudopotentials generated from ionized configurations tend to be less accurate. Finally one can generate pseudopotentials with several different reference energies,[9] in this way by-passing the Schrödinger equation inversion step, but that requires the rewriting of the computer codes for the bulk that rely on the traditional pseudopotential form.

In this work we overcome this limitation of traditional pseudopotentials in general and of the TM scheme in particular by developing a pseudopotential generation scheme which allows the inclusion of semicore states, while keeping the traditional semilocal form of the pseudopotential, which means they can be used without further changes in bulk computational codes. The strategy constitutes a generalization of the ideas underlying the TM method which have been repeatedly shown to provide a highly efficient pseudopotential generation scheme. Application of this scheme—which will be denoted in the following as the multireference pseudopotential (MRPP)—to selected, representative elements shows that the present method is not only capable of producing high-quality results for diatomics and bulk matter—when benchmarked against AE results—but also that one can now use semicore electrons efficiently in a PW framework.

This paper is organized as follows. After a brief review of general pseudopotential theory in Sec. II, Sec. III will review the TM method, which will be generalized to the MRPP recipe in Sec. IV, in order to incorporate semicore electrons. We test the method in Sec. V for several $3d$ transition metals. We choose the rather unfavorable (in a PW sense) case of dimers as well as the more suitable bulk phases of these elements and compare the results obtained with the new pseudopotentials with those originating from AE calculations as well as with those associated with the standard TM pseudopotentials. In Sec. VI we summarize the main conclusions of this work. The method developed here is implemented in a code which, similarly to what happens for many years with the TM, is freely available.[16]

II. GENERAL PSEUDOPOTENTIAL THEORY

The majority of the pseudopotentials currently used in electronic structure calculations are generated from AE atomic calculations. Within DFT this is done by assuming a spherical approximation for the potential in the self-consistent solution of the radial Kohn-Sham equation

$$\left[-\frac{1}{2}\frac{d^2}{dr^2}+\frac{l(l+1)}{2r^2}+V[\rho;r)\right]rR_{nl}(r)=\epsilon_{nl}rR_{nl}(r), \quad (1)$$

where $V[\rho;r)$ is the self-consistent one electron potential

$$V[\rho;r)=-\frac{Z}{r}+V_H[\rho;r)+V_{\mathrm{XC}}^{\mathrm{LDA}}[\rho(r)], \quad (2)$$

$\rho(r)$ is the sum of the electron densities associated with the occupied wave functions $R_{nl}(r)$, $V_H[\rho;r)$ is the Hartree potential, and $V_{\mathrm{XC}}^{\mathrm{LDA}}[\rho(r)]$ is the local density approximation for the exchange-correlation potential. The notation $V_H[\rho;r)$ indicates a functional dependence on the density ρ. Here and elsewhere in the article we use atomic (Hartree) units unless otherwise indicated.

Most pseudopotentials are then constructed such that they satisfy four general conditions.[3,6,8]

(1) The valence (the principal quantum number n is here omitted for simplicity) pseudo-wave-functions generated from the pseudopotential should contain no nodes. This stems from the fact that one would like to construct smooth pseudo-wave-functions and therefore the wiggles associated with the nodes are undesirable. This condition will be necessarily superseded in Sec. IV in order to account for semicore states.

(2) The normalized atomic radial pseudo-wave-function (PP) with angular momentum l is equal to the normalized radial AE wave function beyond a chosen cutoff radius r_{cl},

$$R_l^{\mathrm{PP}}(r)=R_l^{\mathrm{AE}}(r) \quad \text{for } r>r_{cl}, \quad (3)$$

or converges rapidly to that value.

(3) The charge enclosed within r_{cl} for the two wave functions must be equal

$$\int_0^{r_{cl}}|R_l^{\mathrm{PP}}(r)|^2r^2dr=\int_0^{r_{cl}}|R_l^{\mathrm{AE}}(r)|^2r^2dr. \quad (4)$$

(4) Of course, the valence AE and PP eigenvalues must be equal,

$$\epsilon_l^{\mathrm{PP}}=\epsilon_l^{\mathrm{AE}}. \quad (5)$$

If a pseudopotential meets the conditions outlined above, it is commonly referred to as a "normconserving pseudopotential."[3] Constructing a pseudo-wave-function that fulfills these requirements can be accomplished using

many different schemes.[6–8] The nonuniqueness of these pseudopotentials is a clear indication of the available variational freedom which can be used at profit to produce a smooth pseudopotential.

Once the pseudo-wave-function is obtained, the screened pseudopotential is then recovered by inversion of the radial Kohn-Sham equation [Eq. (1)]; explicitly,

$$V_{\mathrm{scr},l}^{\mathrm{PP}}(r)=\epsilon_l-\frac{l(l+1)}{2r^2}+\frac{1}{2rR_l^{\mathrm{PP}}(r)}\frac{d^2}{dr^2}rR_l^{\mathrm{PP}}(r). \quad (6)$$

According to Eq. (6), for a nodeless pseudo-wave-function the pseudopotential does not have any singularities, except possibly at the origin. From Eq. (6) we can also see two more important details. Indeed, if we wish the pseudopotential to be continuous, then the pseudo-wave-function must have continuous derivatives up to and including the second derivative. Moreover, if we wish to avoid a hard-core pseudopotential with a singularity at the origin, the pseudo-wave-function must behave as r^l near the origin.

The screening from the valence electrons depends strongly on the environment in which they are placed. If we remove the screening effects of the valence electrons and generate a so-called ionic pseudopotential, we can then use this potential in a self-consistent procedure to determine the electron screening in other environments. This is done by subtracting the Hartree $V_H^{\mathrm{PP}}(r)$ and exchange-correlation $V_{\mathrm{XC}}^{\mathrm{PP}}(r)$ potentials calculated from the valence pseudo-wave-functions from the screened potential to generate an ionic pseudopotential

$$V_{\mathrm{ion},l}^{\mathrm{PP}}(r)=V_{\mathrm{scr},l}^{\mathrm{PP}}(r)-V_H^{\mathrm{PP}}(r)-V_{\mathrm{XC}}^{\mathrm{PP}}(r). \quad (7)$$

A major consequence of the pseudopotential generation procedure just outlined is that each angular momentum component of the wavefunction will see a different potential. The ionic pseudopotential operator is then

$$\hat{V}_{\mathrm{ion}}^{\mathrm{PP}}(r)=V_{\mathrm{ion,local}}^{\mathrm{PP}}(r)+\sum_l V_{\mathrm{non},l}(r)\hat{P}_l, \quad (8)$$

where $V_{\mathrm{ion,local}}^{\mathrm{PP}}(r)$ is the local potential and

$$V_{\mathrm{non},l}(r)=V_{\mathrm{ion},l}^{\mathrm{PP}}(r)-V_{\mathrm{ion,local}}^{\mathrm{PP}}(r) \quad (9)$$

is the nonlocal (or more precisely semilocal) potential for the angular momentum component l, and $\hat{P}_l$ projects out the lth angular momentum component from the wave function. The local potential can in principle be arbitrarily chosen, but since the summation in Eq. (8) will need to be truncated at some value of l, the local potential should be chosen such that it adequately reproduces the atomic scattering for all the higher angular momentum channels.

III. THE TM SCHEME

As our new scheme constitutes a generalization of the TM procedure, we describe first the essential points of the TM, laying the grounds for the generalization to be carried out in the next section. The TM fully complies with the four norm-conservation conditions stated previously, taking advantage of the variational freedom to impose additional constraints which in turn lead to particularly smooth pseudopotentials. The radial part of the pseudo-wave-function is first defined by the equations

$$R_l^{\mathrm{PP}}(r)=\begin{cases} R_l^{\mathrm{AE}}(r) & \text{if } r\geqslant r_{cl}, \\ r^l e^{p(r)} & \text{if } r\leqslant r_{cl}, \end{cases} \quad (10)$$

where $p(r)$ is a polynomial of order six in r^2,

$$p(r)=b_0+b_2r^2+b_4r^4+b_6r^6+b_8r^8+b_{10}r^{10}+b_{12}r^{12}. \quad (11)$$

The seven coefficients of the polynomial are determined from the following seven conditions:[8] (i) norm conservation of charge within an input core radius r_{cl}, (ii)–(vi) continuity of the pseudo-wave-function and its first four derivatives at r_{cl} (which in effect imposes the continuity of $V_{\mathrm{scr},l}(r)$ and its first two derivatives at r_{cl}), and (vii) zero curvature of the screened pseudopotential at the origin. This seventh condition leads to especially smooth pseudopotentials.

The derivatives of the wave function and screened potentials are evaluated from the numerical AE wave function and screened potential using seven-order finite difference formulas, whereas the integrations required to ensure the norm-conservation condition are evaluated numerically. In the final step the screened pseudopotential is obtained by inverting the Kohn-Sham radial equation [Eq. (1)], and in this case Eq. (6) can be written explicitly:

$$V_{\mathrm{scr},l}(r)=\begin{cases} V_{\mathrm{AE}}(r) & \text{if } r\geqslant r_{cl}, \\ \varepsilon_l+\dfrac{l+1}{r}p'(r)+\dfrac{p''(r)+[p'(r)]^2}{2} & \text{if } r\leqslant r_{cl}. \end{cases} \quad (12)$$

IV. THE MRPP SCHEME

In the new formulation we must distinguish between those states of a given l for which there will be a single pseudo-wave-function from those for which there will be more than one pseudo-wave-function. For the former states, the TM scheme will still hold, which means it will be maintained, whereas for the latter states a new scheme must be developed. Since we are interested here in transition metal elements we will, for the sake of simplicity in the notation, give the scheme for those elements, but obviously the scheme is completely general. In the $3d$ transition metals the semicore states are the $3s$ and $3p$ states. Therefore, and for each $l<2$ value, we require that the pseudopotential one wants to generate provides, as a solution of the radial Kohn-Sham equation, nodeless pseudo-wave-functions which match the ''semicore'' orbitals for $r\geqslant r_{cl}$ *and also* single-node pseudo-wave-functions which match the valence orbitals for $r\geqslant r_{cl}$. We achieve this goal by generating the MRPP pseudopotential in the following way.

(1) We start by defining the form of the pseudo-wave-function for the semicore s and p states ($l<2$) as well as to the valence states with $l\geqslant 2$. These pseudo-wave-functions will be nodeless. Explicitly,

$$l<2,\ R_{0,l}^{\mathrm{PP}}(r)=\begin{cases} R_{\mathrm{sc},l}^{\mathrm{AE}}(r) & \text{if } r\geqslant r_{cl}, \\ r^l e^{q(r)} & \text{if } r\leqslant r_{cl}, \end{cases} \tag{13}$$

$$l\geqslant 2,\ R_{0,l}^{\mathrm{PP}}(r)=\begin{cases} R_{v,l}^{\mathrm{AE}}(r) & \text{if } r\geqslant r_{cl}, \\ r^l e^{p(r)} & \text{if } r\leqslant r_{cl}, \end{cases} \tag{14}$$

where $p(r)$ is a polynomial of order 6 in r^2 as written in Eq. (11), and $q(r)$ is a polynomial of order 9 in r^2,

$$q(r)=c_0+c_2r^2+c_4r^4+c_6r^6+c_8r^8+c_{10}r^{10}+c_{12}r^{12}+c_{14}r^{14}+c_{16}r^{16}+c_{18}r^{18}. \tag{15}$$

The index 0 in $R_{0,l}^{\mathrm{PP}}$ explicitly indicates that these are nodeless pseudo-wave-functions for which the inversion of the Kohn-Sham equation is possible. $R_{\mathrm{sc},l}^{\mathrm{AE}}(r)$ are the inner-shell (semicore) AE wave functions with $l<2$, whereas for $l\geqslant 2$ we can use the outer-shell (valence) AE wave functions, denoted by $R_{v,l}^{\mathrm{AE}}(r)$.

We exploit the variational freedom in the three additional polynomial coefficients c_i in $q(r)$ to supplement the standard set of seven conditions enumerated in the previous section, and which are applicable to the nodeless semicore pseudo-wave-functions, with a group of three additional conditions applied to the single-node valence pseudo-orbitals with $l<2$:

$$\text{(viii)}\quad R_{1,l}^{\mathrm{PP}}(r_{cl})=R_{v,l}^{\mathrm{AE}}(r_{cl})\quad (l<2) \tag{16}$$

$$\text{(ix)}\quad \int_0^{r_{cl}}|R_{1,l}^{\mathrm{PP}}(r)|^2r^2dr=\int_0^{r_{cl}}|R_{v,l}^{\mathrm{AE}}(r)|^2r^2dr\quad (l<2) \tag{17}$$

$$\text{(x)}\quad \varepsilon_{1,l}^{\mathrm{PP}}=\varepsilon_{v,l}^{\mathrm{AE}}\quad (l<2). \tag{18}$$

As a result, we obtain a system of linear equations for the new unknowns c_2, c_4, c_6, c_8, and c_{10}, which, in turn, become implicit functions of the remaining five unknowns c_0, c_{12}, c_{14}, c_{16}, and c_{18}. These coefficients, in turn, are the solution of the following nonlinear system of equations:

$$\begin{cases} \ln\int_0^{r_{cl}}r^{2(l+1)}e^{2q(r)}dr-\ln\int_0^{r_{cl}}|R_{\mathrm{sc},l}^{\mathrm{AE}}(r)|^2r^2dr=0, \\ c_2^2+c_4(2l+5)=0, \\ R_{1,l}^{\mathrm{PP}}(r_{cl})-R_{v,l}^{\mathrm{AE}}(r_{cl})=0, \\ \ln\int_0^{r_{cl}}|R_{1,l}^{\mathrm{PP}}(r)|^2r^2dr-\ln\int_0^{r_{cl}}|R_{v,l}^{\mathrm{AE}}(r)|^2r^2dr=0, \\ \varepsilon_{1,l}^{\mathrm{PP}}-\varepsilon_{v,l}^{\mathrm{AE}}=0. \end{cases} \tag{19}$$

We solve this system of equations numerically using the multidimensional secant method of Broyden.[17] As with any nonlinear system of equations we need a good starting point. This is provided by the TM method applied to the semicore states, that is, we start from $q(r)=p(r)$ which means that $c_{14}=c_{16}=c_{18}=0$. By solving the nonlinear problem we determine numerical values for the coefficients c_0, c_{12}, c_{14}, c_{16}, and c_{18}, which in turn enables us to obtain explicit values for the remaining coefficients.

TABLE I. Values utilized in the calculations leading to the results discussed in the main text, are shown for each of the elements considered. All distances are in Bohr, and energies in Hartree. In a PW calculation of molecules, the size of the unit cell should be large enough so that the atoms in a given cell do not interact with those in any of the neighboring cells. In all cases, r_{cut} specifies the l-dependent values for the cutoff radii used in the construction of the different pseudopotentials. Three values are tabulated for each pseudopotential corresponding, from left to right, to the cutoff radii used for the s, p, and d components, respectively. For the MRPP pseudopotentials, and for each l value, only one value for the cutoff radius has been used, although this is by no means compulsory (see main text for details).

Element	Ti	Cu
r_{cut}(TM)	2.54 2.96 2.25	2.08 2.30 2.08
r_{cut}(MRPP)	1.75 1.75 1.65	1.50 1.50 1.80
cell size (dimer)	27	27
E_{cut}(dimer)	40	40
E_{cut}(bulk)	71	64

V. RESULTS AND DISCUSSION

In order to assess the reliability of the MRPP scheme, we tested the pseudopotentials for all transition metals (plus copper) in two extreme coordination number cases: homonuclear dimers and the bulk solid. Here we only show the results for two elements, titanium and copper, selected from the two sides of the $3d$ series. All calculations were performed in the local density approximation to DFT, and the exchange-correlation functional used corresponds to the Perdew and Zunger parametrization[18] of the quantum Monte Carlo results obtained by Ceperley and Alder.[19] As is well known, the LDA does not describe the magnetization of $3d$ transition metals very well, and the multiplets of transition metal dimers are difficult to converge to self-consistency. The objective of our work is the accuracy of the pseudopotential approximation and therefore how close it reproduces the corresponding AE results. By restricting ourselves to the LDA and using a temperature broadening of 2000 K for state occupancy, we simplify our computational task while focussing on the difference between the pseudopotential and the corresponding AE results, which is the ultimate benchmark for any pseudopotential approximation.

In spite of numerous constraints imposed in the construction of the pseudo-wave-functions, there is still variational freedom to construct the pseudopotentials. This reflects itself in, e.g., the different possibilities for the choice of the cutoff radii. For each element we took one single value of r_{cut} for each l value which, in addition to ensuring the inexistence of ghost states upon the Kleinman and Bylander tranformation,[20] also optimizes the results for the homonuclear dimers. The final choices for r_{cut} are given, in atomic units, in Table I, together with other relevant parameters of the PW calculation. Input files to generate all $3d$ transition

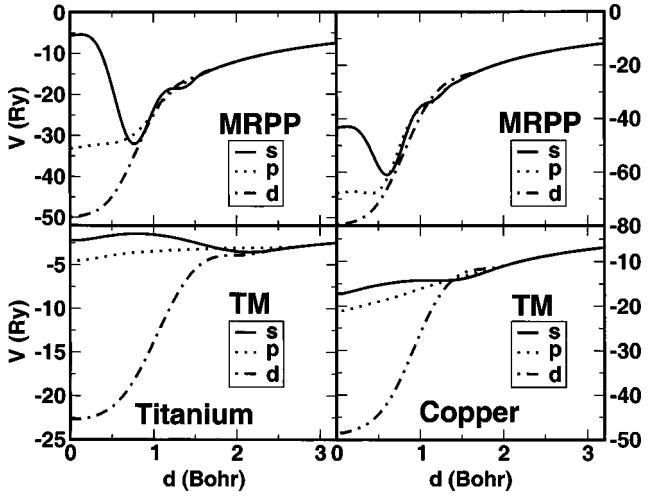

FIG. 1. Comparison of different pseudopotentials for titanium and copper. The MRPP pseudopotentials are displayed (upper panels) in comparison with the standard TM pseudopotentials (lower panels) for titanium (left panels) and copper (right panels). In each panel the *s* component is drawn with a solid line, the *p* component is drawn with a a dotted line, and the *d* component is drawn with a dash-dotted line.

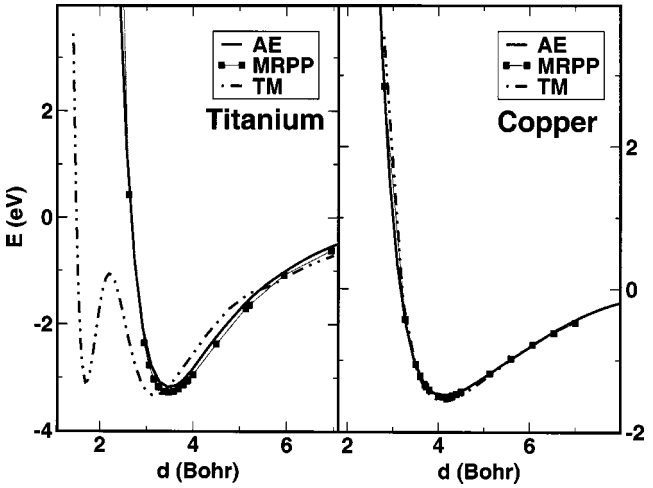

FIG. 2. Cohesive energy of dimers. The cohesive energy of homonuclear dimers of titanium (left panel) and copper (right panel) have been computed as a function of atomic separation and at three levels of description of each constituent atom, leading to three curves per panel: AE (solid lines), MRPP (solid squares), and TM (dash-dotted lines). The MRPP results exhibit an overall agreement with the AE results, eliminating the spurious double well potential obtained for titanium at the TM level.

metal pseudopotentials are freely available, together with the pseudopotential generation code.[16]

Figure 1 shows a comparison between the MRPP and the TM pseudopotentials for the elements explicitly considered in this work. Because of the higher ionic charge in the case of the MRPP, the associated pseudopotential is significantly deeper than the TM, also to be able to accomodate not only the semicore but also the valence pseudo-wave-functions. Of course this more pronounced spatial variation of the MRPP as compared to the TM reflects itself in the higher cutoff energies required to ensure full convergence of the PW calculations. Nevertheless, the values used for the energy cutoff are still reasonable, as shown in Table I. The cutoff energy is larger for the bulk than for the dimer calculations, since we are using the internal pressure in the optimization of the cell shape.[21] For the dimers we computed the cohesive energy as a function of the interatomic distance, shown in Fig. 2, whereas for the bulk phase we computed the equilibrium lattice parameters, shown in Table II. For each of these quantities we provide results obtained at three levels of description: The present MRPP, the traditional TM results, and the AE results obtained with the ADF package[22] for the dimer and taken from the literature for the bulk. The agreement between the MRPP results and the AE results is excellent in all cases, the MRPP providing an overall improvement with respect to the TM results.

In the case of the Ti dimer the improvement is dramatic, as can be judged from Fig. 2. The curve predicted by the TM pseudopotential has a double well with a second low lying minimum at 1.7 Bohr, in a region where the AE curve is strongly repulsive. That is a clear failure of the traditional pseudopotential for the Ti dimer. The inclusion of the semicore states and the valence states in the pseudopotential corrects the problem, and the curve predicted by the MRPP falls on top of the AE curve. This double well feature is also present for scandium and vanadium at the TM level, disappearing at the MRPP level. It should be pointed out that this double well is unphysical. Indeed, at the distances of the shorter minimum there is a sizeable overlap of the semicore electrons of the two systems with consequent large Pauli repulsion which is absent in the TM pseudopotential, but accounted for in both the MRPP and AE calculations. In the bulk, the double well feature observed for the titanium dimer does not occur since for the large coordination number of bulk, δ bonds do not appear and interatomic distances are never so short as for the dimer.

For copper both the TM and MRPP pseudopotentials reproduce closely the AE curve. The $3s$ and $3p$ states are much deeper in copper and can be safely treated as core states, as far as structural properties are concerned. However, for the calculation of excitation energies, there is some indication of GW calculations that they cannot be neglected. Our new scheme would allow their inclusion in such calculations.[13]

TABLE II. The calculated equilibrium lattice constants are compared for three different methods for bulk Ti and Cu. The TM and MRPP results were computed with the parameters specified in Table I, whereas the AE results for titanium were taken from Ref. 23 and those for copper were taken from Ref. 24.

Element	Lattice type		TM	MRPP	AE
Ti	hcp	*a*	5.46	5.42	5.42
		c	8.73	8.60	8.60
Cu	fcc		6.74	6.72	6.73

VI. CONCLUSIONS

We have developed a systematic scheme to generate first-principles, transferable norm-conserving pseudopotentials which, while explicitly including semicore electrons which are known to play an important role in the physics and chemistry of transition metal atoms, are still sufficiently smooth to enable the efficient and accurate simulation of both low- and high-dimension materials involving these types of elements. The scheme developed uses the TM as a starting point, thereby taking advantage of the smoothing constraints already developed in the TM scheme. The results obtained in the two limiting bonding situations corresponding to homonuclear dimers and bulk solid show, in all cases, excellent agreement between the predictions of the MRPP and those resulting from benchmark AE calculations of the same systems.

ACKNOWLEDGMENTS

Financial support from the Portuguese Foundation for Science and Technology under Contract No. POCTI/FIS/10019/98 and POCTI/36279/99 is gratefully acknowledged.

[1] E. Fermi, Nuovo Cimento **11**, 157 (1934).
[2] J. C. Phillips and L. Kleinman, Phys. Rev. **116**, 287 (1959).
[3] D. R. Hamann, M. Schlüter, and C. Chiang, Phys. Rev. Lett. **43**, 1494 (1979).
[4] G. P. Kerker, J. Phys. C **13**, L189 (1980).
[5] A. Zunger and M. L. Cohen, Phys. Rev. B **18**, 5449 (1978).
[6] G. B. Bachelet, D. R. Hamann, and M. Schlüter, Phys. Rev. B **26**, 4199 (1982).
[7] D. R. Hamann, Phys. Rev. B **40**, 2980 (1989).
[8] N. Troullier and José Luís Martins, Phys. Rev. B **43**, 1993 (1991).
[9] D. Vanderbilt, Phys. Rev. B **41**, 7892 (1990).
[10] For a review see, e.g., W. E. Pickett, Comput. Phys. Rep. **9**, 115 (1989); R. M. Martin (unpublished).
[11] In the original sense soft and hard pseudopotentials distinguished between pseudopotentials that were finite or diverged at the origin. Currently soft pseudopotentials have the meaning described in the text.
[12] J. A. Alonso, Chem. Rev. (Washington, D.C.) **100**, 637 (2000).
[13] Andrea Marini, Giovanni Onida, and Rodolfo del Sole, Phys. Rev. B **64**, 195125 (2001); Phys. Rev. Lett. **88**, 016403 (2002); *ibid.* **48**, 1425 (1982).
[14] Th. Starkloff and J. D. Joannopoulos, Phys. Rev. B **19**, 1077 (1979).
[15] D. M. Bylander and L. Kleinman, Phys. Rev. B **29**, 2274 (1984).
[16] URL: http://aloof.cii.fc.ul.pt/AGI/
[17] W. H. Press, S. A. Teukolsky, W. T. Vetterling, and B. P. Flannery, *Numerical Recipes in Fortran 77* (Cambridge University Press, Cambridge, 1989), Sec. 9.7.
[18] J. P. Perdew and A. Zunger, Phys. Rev. B **23**, 5048 (1981).
[19] D. M. Ceperley and B. J. Adler, Phys. Rev. Lett. **45**, 566 (1980).
[20] L. Kleinman and D. M. Bylander, Phys. Rev. Lett. **48**, 1425 (1982).
[21] I. Souza and J. L. Martins, Phys. Rev. B **55**, 8733 (1997).
[22] G. te Velde and E. J. Baerends, J. Comput. Phys. **99**, 84 (1992).
[23] Z-W Lu, D. Singh, and H. Krakauer, Phys. Rev. B **36**, 7335 (1987).
[24] L. G. Wang and M. Šob, Phys. Rev. B **60**, 844 (1999).